

MICROMECHANICS-BASED MODELS FOR FRACTURE AND BREAKOUT AROUND THE MINE-BY TUNNEL

P. A. CUNDALL, D. O. POTYONDY and C. A. LEE
Itasca Consulting Group, Inc., Minneapolis, Minnesota, USA

1 INTRODUCTION AND BACKGROUND

The mine-by tunnel [1, 2] at the Underground Research Laboratory (URL) has exhibited breakout, notch formation and associated seismic emissions. Although such breakout is a common occurrence in tunnels and boreholes, it was unexpected in the mine-by tunnel because the maximum induced stress at the tunnel surface has been calculated to be considerably lower than the measured uniaxial strength of core samples taken from the surrounding rock. Numerical modeling of the failure process must (1) reproduce the specific shape of the notch (apparently a cusp-like object), and (2) provide a match between the numerical values obtained from both the field and the model, which include rock-mass properties, near-tunnel displacements and far-field stresses that cause failure.

A modeling approach that treats rock as a heterogeneous material is described in this paper. To an important degree, mechanisms occurring at the microscopic level are assumed to influence macroscopic behavior. The modeling approach is especially applicable to situations in which the stress state is nearly uniaxial — e.g., at the surface of an underground excavation. Surface-parallel cracking is often observed for such cases. This phenomenon is difficult to explain without invoking microscopic mechanisms that, for example, induce local tension and/or local buckling.

In this paper, a micromechanical model for rock is described first, followed by the presentation of a simple constitutive model based on idealizations of some observed mechanisms. The resulting constitutive model is then used within a continuum code to simulate failure in the mine-by tunnel.

2 BEHAVIOR OF BONDED-PARTICLE MODELS

Rock is a heterogeneous material that can develop numerous microcracks during the loading process before visible macrocracks appear. Many numerical models of rock treat the material as a uniform continuum within which a few dominant macrocracks can propagate. An alternative approach, which may better express the heterogeneous nature of rock, treats the material as a collection of separate particles bonded together at their contact points. Under load, this material can develop “microcracks” as individual bonds break; the microcracks can then coalesce into contiguous bands or strings that resemble macrocracks. Figure 1 illustrates the physical basis of this conceptual model.

The bonded-particle approach is described in some detail by Potyondy et al. [3] and compared to similar methods that idealize solid material as a lattice of structural units (bonds, springs, beams, etc.); only a brief summary is provided here. The bonded-particle model consists of a dense packing of arbitrarily sized circular particles that are bonded together at their contact points and simulated by the distinct-element method [4], which embodies an explicit, time-marching scheme to solve the equations of motion for distinct particles. In the numerical experiments reported here, each bond behaves like a pair of elastic springs acting in the normal and shear directions of relative motion. When either a tensile normal- or shear-force limit is reached, the bond breaks and can carry no tension thereafter. However, it can still support a compressive normal force and a shear force of magnitude less than μF_n , where μ is the friction coefficient and F_n is the normal force (positive for compression).

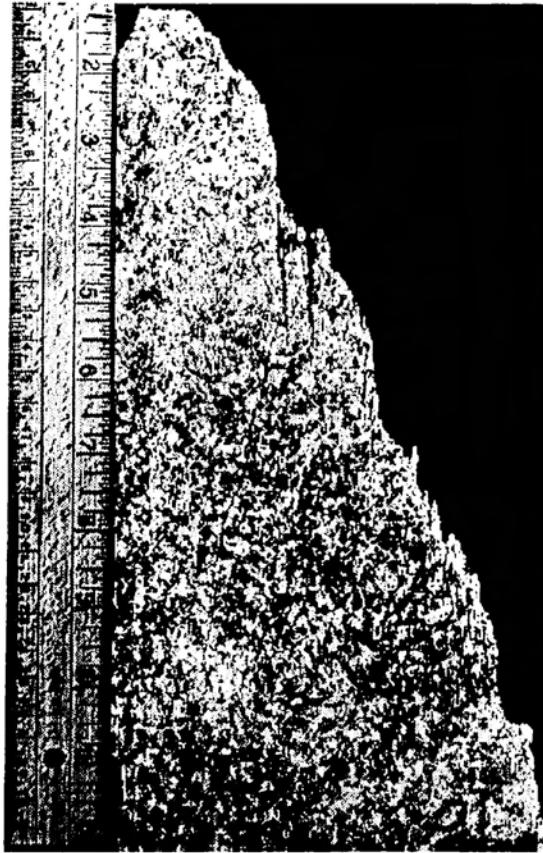


Figure 1 Failure surface developed in 200 mm diameter sample of Lac du Bonnet granite (Note the short axial cracks that form adjacent to the failure surface.)

PFC^{2D} [5] is used to perform a calibration procedure on samples composed of the bonded material described above, with the purpose of matching numerically derived synthetic properties with laboratory properties of Lac du Bonnet granite. Before performing uniaxial and biaxial tests on the samples, procedures are applied to ensure that each sample contains a small number of disconnected particles and that the locked-in forces are small compared to the forces that will be generated during loading. A portion of a typical sample before loading is shown in Figure 2, where each bond is drawn as a line connecting the centers of bonded particles.

The computed stress-strain responses for four tests with confining stresses, σ_0 , of 0, 20, 40, and 80 MPa are presented in Figure 3(a), in which the deviatoric stress (defined as the axial stress minus the confining stress) is plotted versus the axial strain. The effect of the confinement is to increase the peak strength; it has little effect on the elastic modulus. This behavior is similar to the laboratory behavior of granite.

The breaking of a bond in the *PFC*^{2D} model can be interpreted as the formation of a microcrack oriented in a direction perpendicular to the line joining the centers of the two parent particles. The microcracks formed during the four stages (defined in Figure 3(a)) of the uniaxial test are shown in Figure 4. The majority of the microcracks are aligned with the direction of load application. The cracking is distributed randomly throughout the sample during the pre-peak region (stages A and B) and then begins to localize in the lower half of the specimen during the peak region (stage C). Localization and the rate of microcrack formation become extreme during the post-peak region (stage D), at which time a diagonal band of microcracks develops. The total number of microcracks (dark solid line) is plotted versus axial strain in Figure 3(b). In this plot, the microcracks formed as the result of the tensile normal- or shear-force limit being exceeded are shown by the light solid and dashed lines, respectively.

The bonded-particle model described here reproduces many aspects of rock behavior, but other idealizations of the microstructure may be preferable in some cases. For example, Napier and Peirce [6] show that different grain geometries lead to different patterns of crack coalescence.

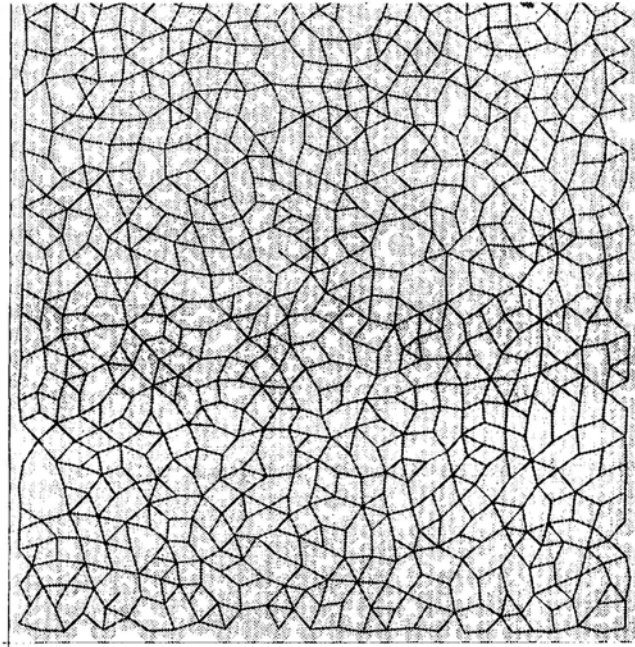


Figure 2 *Particles and contact bond structure in lower portion of sample prior to loading [Potyondy et al. [3], Fig. 2]*

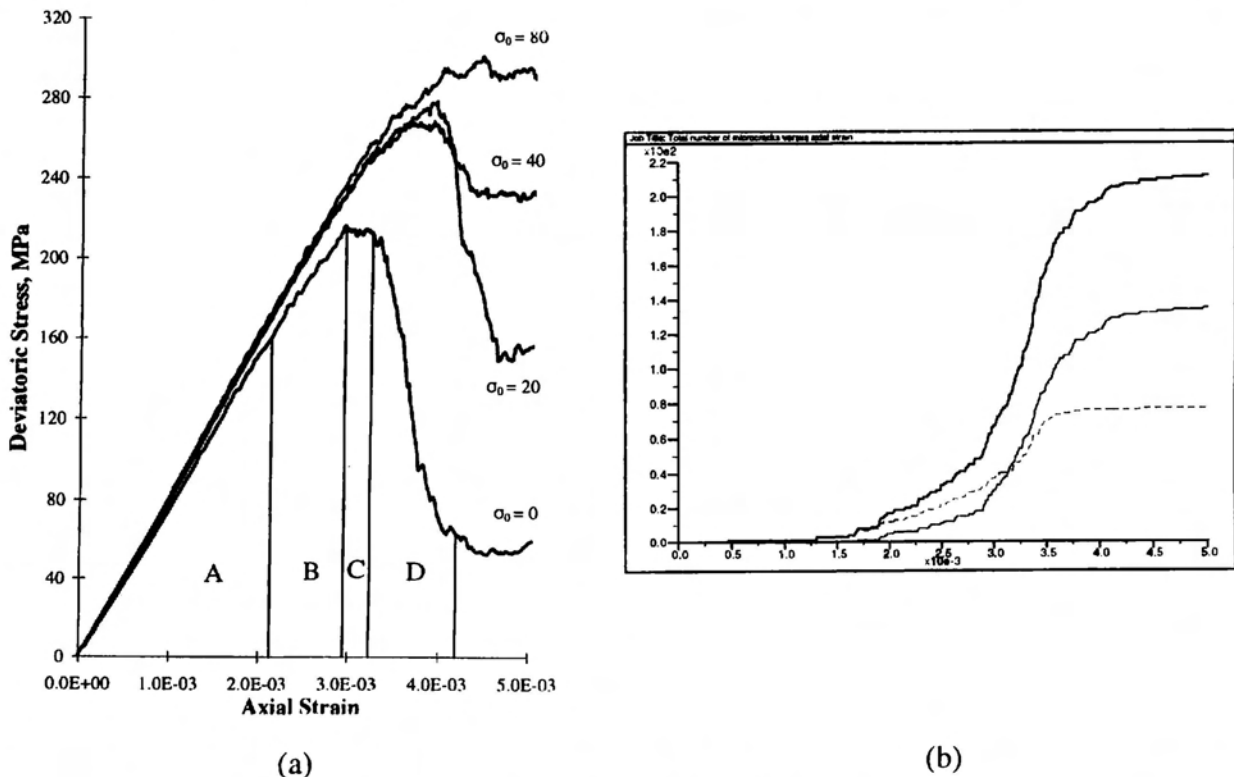


Figure 3 (a) *Deviatoric stress versus axial strain for four tests with confining stresses of 0, 20, 40 and 80 MPa [Potyondy et al. [3], Fig. 4]; (b) total number of microcracks versus axial strain (top solid line)*

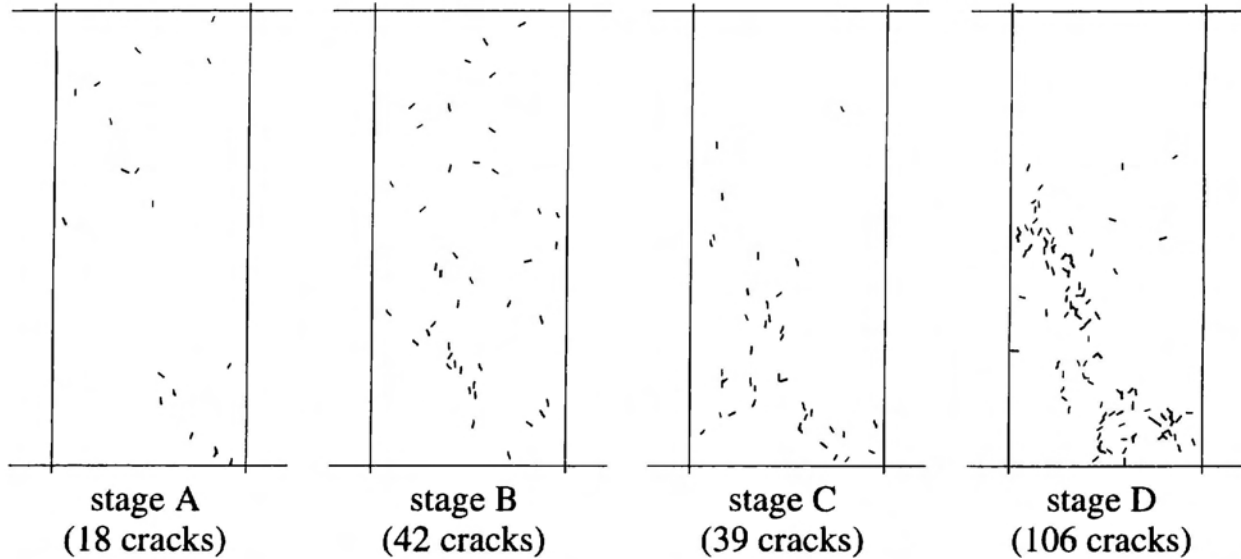


Figure 4 Cracks formed during each of the first four stages of the uniaxial test [Potyondy et al. [3], Fig. 5]

3 A CONSTITUTIVE MODEL BASED ON MICROMECHANICS

Under uniaxial loading conditions, Lac du Bonnet granite develops microcracks aligned parallel with the applied stress, as can be seen in Figure 1; this phenomenon may be termed “extension fracturing.” Such axially aligned microcracks cannot form in a perfectly homogeneous material, because there is no means to induce tension or shear; however, such microcracks do form in the bonded-particle model. One formation mechanism is shown in Figure 5(a), in which a group of four circular particles are forced apart by axial load, causing the restraining bond to experience tension. These axially aligned “microcracks” occur during the early loading stages of compression tests on bonded assemblies of circular particles — see Figure 4. Similar crack-inducing mechanisms occur even when different conceptual models for rock microstructure are used. For example, “wedges” and “staircases” also induce local tension, if angular grains replace circular grains — see Figure 5(b and c).

In order to develop a constitutive model, we can generalize the failure mechanism by envisaging the material as a uniform lattice of rigid, pin-jointed bars connected by horizontally aligned springs, as shown in Figure 5(d). Grain bonding is represented by the springs, each of which carries a tension force, T . If we assume that T is constant at yield, the lattice becomes a mechanism in which the nodal velocities are related by

$$\dot{u}_1 \cos \theta = -\dot{u}_3 \sin \theta \quad (1)$$

Denoting the corresponding strain rates by \dot{e}_1^p and \dot{e}_3^p (where superscript p indicates “plastic”, since the state is one of steady motion, or flow), we obtain

$$\frac{\dot{e}_1^p}{\dot{e}_3^p} = \frac{-\dot{u}_1/L \cos \theta}{-\dot{u}_3/L \sin \theta} = -\tan^2 \theta \quad (\text{derived flow rule}) \quad (2)$$

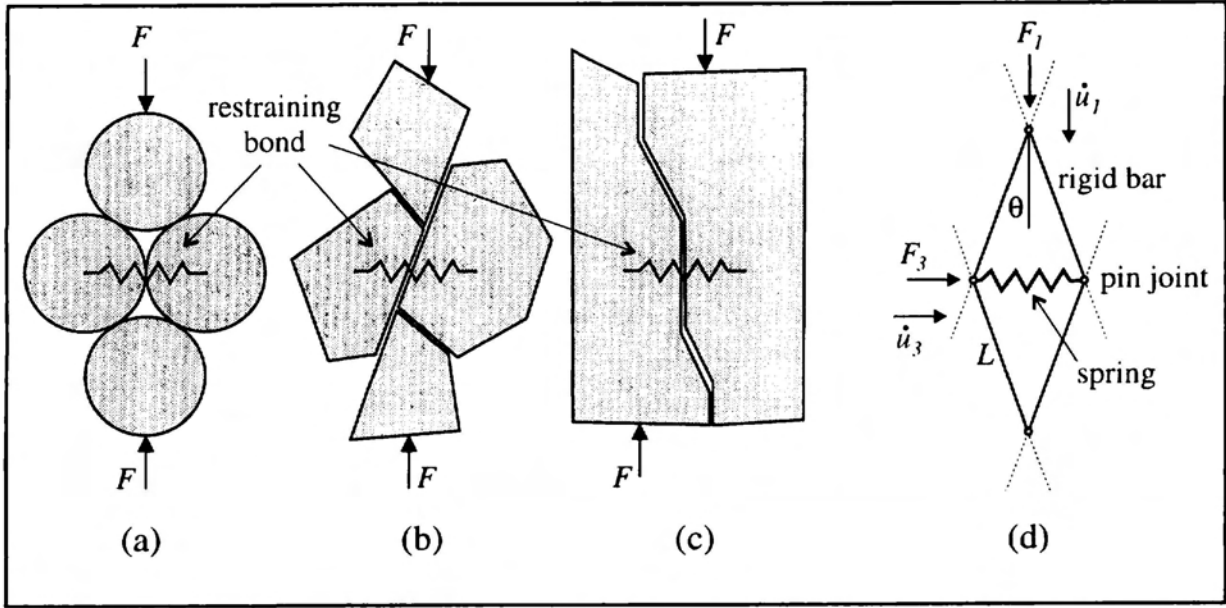


Figure 5 Physical mechanisms for axial cracking (a–c), and lattice idealization (d)

Equation (2) is a flow rule that can be used directly in a plasticity formulation. The parameter θ can be expressed in terms of the forces acting on the structure shown in Figure 5(d) by enforcing equilibrium at the joints to obtain

$$F_1 \tan \theta = F_3 + T \quad (3)$$

The average stresses, σ_1 and σ_3 , can be expressed in terms of the corresponding forces, F_1 and F_3 , as

$$\sigma_1 = -\frac{F_1}{2L \sin \theta} \quad \sigma_3 = -\frac{F_3}{2L \cos \theta} \quad (4)$$

In this and all succeeding equations, tensile stresses are positive. If the bond strength is expressed in stress units as σ_b , then $T = \sigma_b 2L \cos \theta$ at failure. Substituting both this relation and Eq. (4) into Eq. (3) yields

$$\sigma_1 \tan^2 \theta = \sigma_3 - \sigma_b \quad (\text{derived yield condition}) \quad (5)$$

Equation (5) is a yield condition. In plasticity formulations, there are two main components: a flow rule and a yield condition. For the case of extension fracturing, the former is believed to be responsible for axial splitting, because it leads to the large volumetric expansions that are observed in uniaxial tests. We therefore use the flow rule derived from micromechanics (given by Eq. (2)), but use a “standard” yield condition. The Hoek-Brown criterion [7] for rock failure is supported by considerable experimental and field evidence and is given by

$$\sigma_1 = \sigma_3 - \sqrt{s\sigma_c^2 - \sigma_3\sigma_c m} \quad (\text{Hoek-Brown failure criterion}) \quad (6)$$

where s and m are dimensionless material parameters, and σ_c is equal to the uniaxial compressive strength when $s = 0$. We determine θ by asserting that the two criteria given by Eqs. (5) and (6) are identical; this equality implies that the lattice angle θ depends on stress. The physical interpretation of this assertion is that (1) forces are localized in chains that are oriented, on average, at the angles necessary for equilibrium, and (2) when the stress ratio changes, the force-chain pattern also changes. It is generally observed in numerical tests on granular assemblies that small lattice angles correspond to high stress ratios.

Whenever the constitutive model is invoked, the lattice angle, θ , is evaluated based on the current stresses according to Eq. (5) but with the bond strength σ_b determined by the condition that σ_b must be equal to σ_3 when $\sigma_1 = 0$. Using Eq. (6), for the case of $\sigma_1 = 0$,

$$\sigma_b \equiv \sigma_3 = \frac{\sigma_c}{2} \left(\sqrt{m^2 + 4s} - m \right) \quad (7)$$

The components of the plasticity formulation are now in place. We compute trial elastic principal stresses based on the prescribed strain increments and elastic constants. If the yield criterion (given by Eq. (6)) is violated by these stresses, then the strain increments are assumed to be composed of elastic and plastic parts:

$$\Delta e_i = \Delta e_i^e + \Delta e_i^p \quad (8)$$

Using Eqs. (2), (6) and (8), we can solve for a final set of stresses such that all conditions are satisfied exactly — no iterations are necessary. The full derivation is given by Cundall [8].

The conceptual model underlying the plasticity formulation is a population of bonds yielding in the minor principal-stress direction, with no drop in strength. However, we may imagine that more and more bonds break as straining continues. If a bond is regarded as a spring defined by the unit vector n_i directed along its length, then the development of progressive cracking (damage) may be quantified by a crack tensor. In the formulation described by Oda et al. [9], the crack tensor depends on crack lengths as well as crack orientations. Here, we propose a crack tensor, F_{ij} , for which the magnitude depends on accumulated plastic strain in the minor principal direction:

$$\Delta F_{ij} = \Delta e_3^p n_i n_j / \kappa \quad (9)$$

The unit vector n_i is parallel to the instantaneous direction of minor principal stress and corresponds to a notional crack with normal n_i . For example, a crack tensor with a non-zero component F_{11} would correspond to cracks aligned vertically in Figure 5(d). The variable κ is a softening parameter that is equal to the plastic strain necessary for the crack tensor to reach a value of unity, for straining in a given direction. Although the magnitude of F_{ij} may exceed unity, this state is regarded as “fully cracked,” and any value above one is regarded as equal to one.

In order to incorporate the crack tensor into the strength formulation, we note that parameter s in the Hoek-Brown criterion (given by Eq. (6)) corresponds with a degree of brokenness such that intact material is represented by $s = 1$ and fully broken material by $s = 0$. (Note that uniaxial strength is zero for $s = 0$, although the yield surface is still curved.) If s were reduced progressively from 1 to 0, the material would appear to soften isotropically. To account for the directional effect of cracking, we compute the apparent strength on the plane with a normal vector in the minor principal stress direction of n_i :

$$s = \max(0, 1 - F_{ij}n_in_j) \quad (10)$$

The negative sign in Eq. (10) accounts for the fact that s is a “strength” while the crack tensor records “weakness.” The formulation is similar to that used to obtain normal traction on a plane from a given stress tensor. The value of s computed according to Eq. (10) is used in Eq. (6). The current anisotropic state of damage in the material is equal to F_{ij} , which can be plotted as a tensor field indicating crack intensity and direction.

The constitutive model has been exercised by modeling samples in a simulated testing environment [8]: surface spalling is observed under uniaxial conditions and a transition to shear localization is observed as the confining stress is increased. The spalling behavior is attributed to the high dilatation exhibited by the model under low confinement.

4 TUNNEL SIMULATIONS WITH A CONTINUUM MODEL

FLAC [10] is used by Cundall [11] to model a two-dimensional section of the mine-by tunnel under conditions of double symmetry, using the constitutive model summarized in Section 3. The model boundaries are located at distances from the centerline equal to ten times the tunnel radius (1.75 m). A portion of the grid is shown in Figure 6(a): a fine grid is used near the tunnel, with the grid becoming progressively coarser as the outer boundary is approached. The parameters used in the simulation reported here are listed in Table 1. Note that the value of unconfined compressive strength (σ_c) is lower than the short-term strength of the granite as tested in the laboratory (typically 200 MPa); see Section 5 for discussion on this point.

Table 1 *Parameters used in FLAC simulation*

horizontal field stress	55 MPa
vertical field stress	14 MPa
Young’s modulus	60 GPa
Poisson’s ratio	0.25
softening parameter, κ	0.02 (strain units)
Hoek-Brown parameter, m	30
Hoek-Brown parameter, σ_c	120 MPa

Initial stresses are installed in the grid and applied to the outer boundary, and the model is allowed to reach equilibrium with failure inhibited. Yield is then allowed to occur according to the constitutive model described in Section 3. An erosion criterion is added to the basic formulation as follows: when the scalar damage parameter, s (given by Eq. (10)), becomes zero in any element (i.e., the element is fully cracked), then the element is deleted. The justification for this criterion is that fully cracked material resembles granular material, which either falls out of the failed region or is removed manually. The history of element deletions is shown in Figure 6(b), which illustrates that the process stabilizes after an initial period of rapid failure. At the final state, the tunnel profile exhibits notch formation, shown in Figure 7(a) as a full model (constructed by reflecting the quarter-grid twice about the two lines of symmetry). A close-up view of the new tunnel surface is shown in Figure 7(b), which also shows the field of accumulated crack tensors (given by Eq. (9)). Each tensor is plotted as two lines whose directions and lengths indicate orientations and magnitudes, respectively, of the principal values. In addition, the lines are rotated through 90° to orient them in the same direction as the corresponding cracks. It appears that there is intense damage close to the eroded surface and that there is a localized line of cracks extending into the rock from part-way into the notch. It is interesting to note that similar discrete cracks are observed in the field, in sections that have been cut through notch regions in the mine-by tunnel.

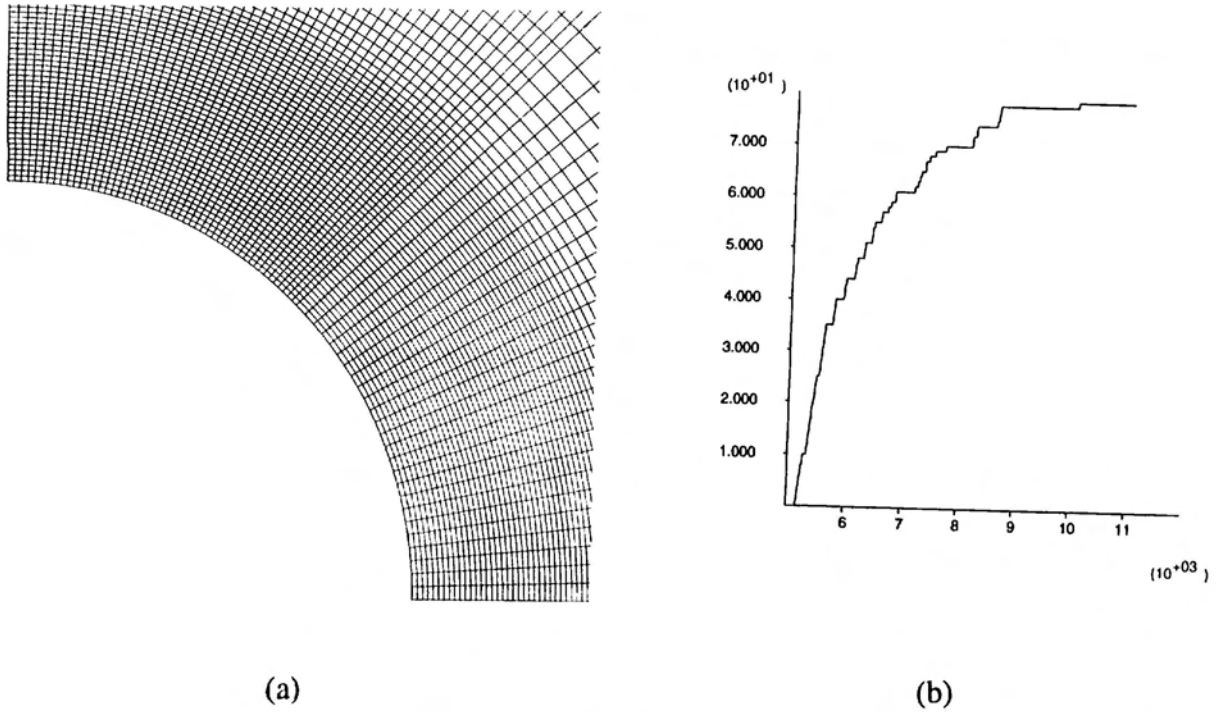


Figure 6 (a) Portion of initial grid containing the tunnel; (b) number of element deletions versus timestep

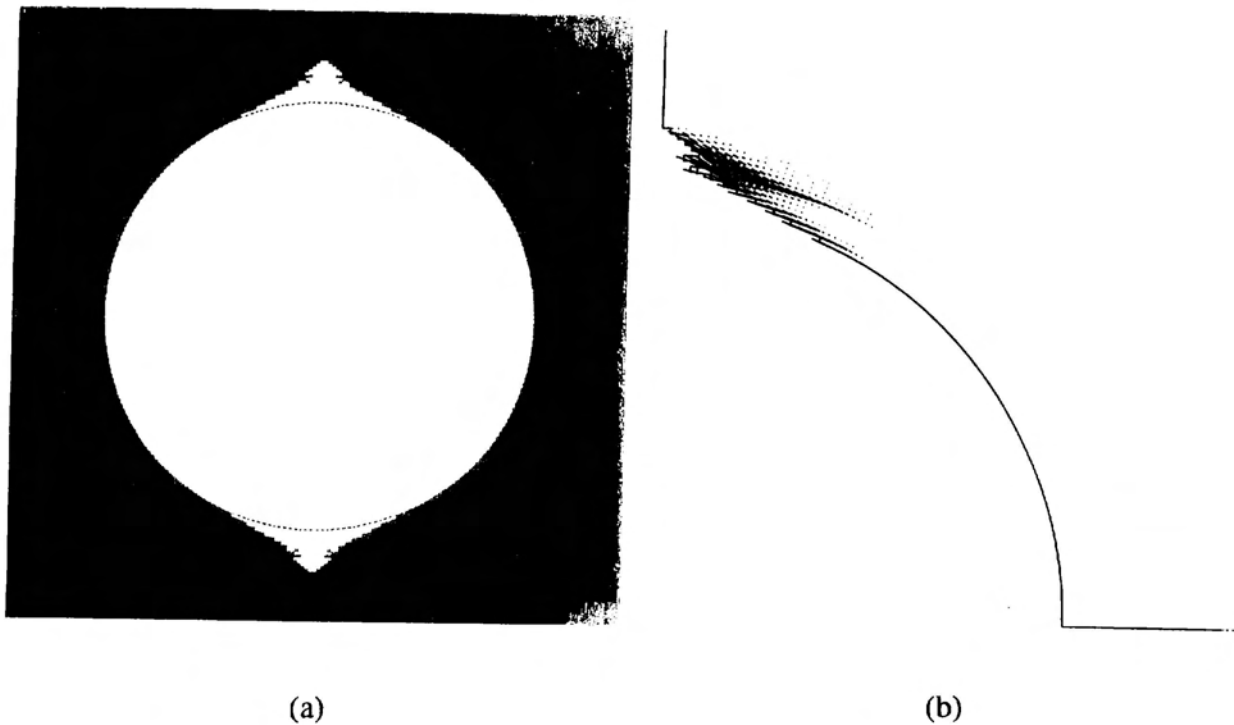


Figure 7 (a) Tunnel profile at final state (Initial tunnel location is indicated by dashed lines.); (b) quarter-section profile and crack tensors rotated through 90 degrees at final state

The extent and form of the simulated notch correspond quite well with structures observed in the mine-by tunnel. In particular, the simulation reveals an active central part, in which the erosion initiates, and an outer part that seems to respond by secondary failure in the form of “flakes.” However, the results are quite sensitive to the value of softening parameter, κ ; further study would be necessary to justify the choice of this parameter on physical grounds.

5 SUMMARY AND CONCLUSIONS

It is possible to reproduce most of the observable characteristics of a rock sample with a bonded-particle model. The model parameters can be calibrated to provide a match with observed modulus, compressive strength, crack-initiation stress and induced volume-changes. Some of the micro-mechanisms revealed by bonded-particle tests can be abstracted and used as the basis of a constitutive model. A continuum simulation of the mine-by tunnel using such a constitutive model captures the notch development and stabilization process well, but it is necessary to assume an artificially low value of rock compressive strength for failure to occur.

There appear to be processes associated with the creation of the mine-by tunnel — in addition to the damage induced by the action of making a circular opening in a plane-strain environment — that cause the rock fabric to be degraded. Some possible candidates for degradation are: locked-in stresses that lead to microcracking upon unloading; pre-cracking of the rock ahead of the face due to stress concentrations and rotations of principal axes of stress; and stress corrosion, which leads to time-dependent cracking. These factors could be incorporated into the continuum model described here by adding initial damage tensors to the grid, but some empirical assumptions would be necessary. Fewer assumptions are needed if the tunnel is simulated directly with the bonded-particle model. This approach has been attempted [12], and preliminary results indicate that stress corrosion is the most likely candidate for material degradation in the mine-by tunnel.

REFERENCES

- [1] READ, R. S. and C. D. MARTIN, “Mine-by experiment final design report,” Atomic Energy of Canada Limited (AECL) Report, AECL-10430, 1991.
- [2] READ, R. S. et al., “Mine-by experiment data summary: Parts 1–9,” AECL Technical Records, TR-577.1 and TR-592 to TR-599, 1993.
- [3] POTYONDY, D. O., P. A. CUNDALL and C. A. LEE, “Modeling rock using bonded assemblies of circular particles,” Second North American Rock Mechanics Symposium, Quebec, Canada, June 1996.
- [4] CUNDALL, P. A. and O.D.L. STRACK, “A discrete numerical model for granular assemblies,” *Géotechnique* **29**(1), 47–65, 1979.
- [5] ITASCA Consulting Group, Inc., *PFC^{2D} (Particle Flow Code in Two Dimensions)*, Version 1.1, ICG, Minneapolis, 1995.
- [6] NAPIER, J.A.L., and A. P. PEIRCE, “Simulation of extensive fracture formation and interaction in brittle materials,” *Mechanics of Jointed and Faulted Rock-MJFR-2*, 63–74, Balkema, Rotterdam, 1995.
- [7] HOEK, E. and E. T. BROWN, *Underground excavations in rock*, Inst. of Mining and Metallurgy, London, 1980.

- [8] CUNDALL P. A. "A preliminary constitutive model for extension fracture based on micromechanics," Report to CSIR Division of Mining Technology, January 1994.
- [9] ODA, M., T. YAMABE and K. KAMEMURA, "A crack tensor and its relation to wave velocity anisotropy in jointed rock masses," *Int. J. Rock Mech. Min. Sci. & Geomech. Abstr.*, **23**(6), 387–397, 1986.
- [10] ITASCA Consulting Group, Inc., *FLAC (Fast Lagrangian Analysis of Continua)*, Version 3.3, ICG, Minneapolis, 1995.
- [11] CUNDALL, P. A. "Modeling of notch formation in the URL mine-by tunnel," Itasca Consulting Group, Inc., Report to AECL, April 1994.
- [12] POTYONDY, D. O., P. A. CUNDALL and C. A. LEE, "Modeling of notch formation in the URL mine-by tunnel: phase II — tunnel simulations," Itasca Consulting Group, Inc., Report to AECL, April 1996.

ACKNOWLEDGEMENTS

We gratefully acknowledge (1) the permission of the Division of Mining Technology (CSIR, Johannesburg, South Africa) to include work on the trellis model that was performed with their support, and (2) the permission of the Underground Research Laboratory (AECL, Pinawa, Canada) to include work with the *PFC^{2D}* and *FLAC* models that was performed with their support.